Journal of Thermal Analysis and Calorimetry, Vol. 86 (2006) 3, 623–629

A DSC STUDY OF THE CRYSTALLIZATION BEHAVIOUR OF POLYLACTIC ACID AND ITS NANOCOMPOSITES

M. Day[*]*, A. Victoria Nawaby and X. Liao*

Institute for Chemical Process and Environmental Technology, National Research Council of Canada, 1200 Montreal Road, Ottawa, Ontario, K1A 0R6, Canada

The isothermal crystallization behaviour of polylactic acid (PLA) and a clay nanocomposite of have been examined using differential scanning calorimetry. The data obtained clearly indicates that the presence of the nanocomposite particles in the composite material influences the crystallization kinetics of the PLA when crystallized both from the solid amorphous state as well as from the melt. When crystallized from the melt the presence of the clay nano-particles appears to be influencing the nucleation and crystal growth rate of the PLA such that the crystallization rate is enhanced by a factor of about 15 to 20. This result is of tremendous significance in identifying the processing window for the production of foamed nanocomposites from PLA. In addition the effect of thermal exposure at 200°C on the crystallization behaviour of these materials has been investigated, with the results suggesting that holding these materials at 200°C for periods of time up to 60 min in an inert atmosphere only has a marginal effect.

Keywords: *crystallization kinetics, clay nanocomposite, polylactic acid, thermal stability*

Introduction

Interest in bio-based products from plant derived chemical feedstocks, such as polylactic acid (PLA) has grown over the last decade due to ever-increasing environmental concerns, as well as the rising cost of petroleum-derived commodity chemicals. Based upon data provided by the National Research Council of the U.S. this interest is anticipated to continue to grow with predictions of 25% of the organic chemicals coming from biofeedstocks by 2020 [1]. Although PLA has been around for several years [2], its widespread commercial acceptance has, until recently, been restricted to high value applications because of costs. However, these costs have been drastically reduced over the last couple of years as modern, more efficient, production technologies have emerged [3, 4]. Another technology which is transforming how we develop and enhance material science is nanotechnology. This has allowed new and innovative materials to be developed such as nanocomposites [5], which have enhanced properties not found in their macroscale counterparts. The incorporation of nanoclay particles into a polymer derived from renewable resources therefore represents a new and innovative approach for the production of more environmentally acceptable advanced materials for the 21st century.

This paper examines the crystallization behaviour of PLA and its nanocomposite containing organically modified layered nano silicate clay particles. This study focuses on the crystallization kinetics of these materials, a factor which is of fundamental importance in understanding and developing the ideal polymer processing conditions. For example the selection of the appropriate temperature during cooling, can significantly effect the development of a specific morphology which in turn can influence the final properties of the material. In addition, since the goal of our research is the production of microcellular foamed nanocomposites there is an added processing complication, namely the solubility of the foaming agent (supercritical CO_2) within the polymer, and the influence of the nano clay particles on bubble-nucleation [6]. Consequently, a fundamental understanding of the kinetics of crystallization is essential to better identify the most appropriate foaming conditions for bubble nucleation and growth to obtain the desired structure, morphology in the final products.

Experimental

The materials evaluated in this study consisted of a nanocomposite sample of polylactic acid designated 'TE-6100' along with the original polylactic acid material used in its fabrication. The sample 'TE-6100'contained 2 mass% of nano clay, that was modified by a proprietary processes to give an intercalated material as can be seen by the X-ray data shown in Fig. 1. Both the samples used in this research were kindly supplied by Unitika Ltd.

The differential scanning calorimetry (DSC) experiments were conducted in sealed aluminum pans

* Author for correspondence: mike.day@nrc-cnrc.gc.ca

1388–6150/$20.00

Akadémiai Kiadó, Budapest, Hungary
Springer, Dordrecht, The Netherlands

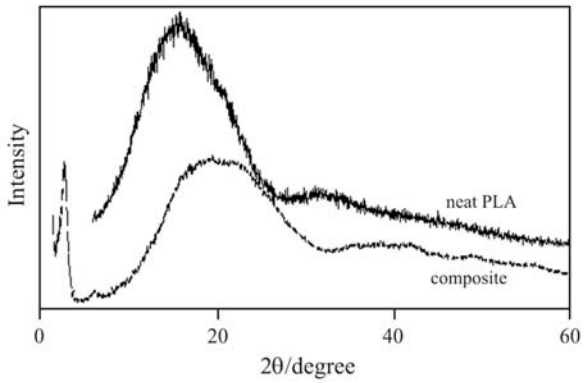

Fig. 1 X-ray patterns for the neat PLA and its nanocomposite

using samples that weighed 6±1 mg, that were determined with ±2 μg precision. All the experiments were conducted in helium (flow rate 50 mL min^{-1}) using a TA Instruments DSC 2910 which was controlled by a TA Instruments 2100. The apparatus was calibrated on a regular basis using indium.

In all the isothermal crystallization kinetic experiments, the samples were first heated to 200°C at a heating rate of 5°C min^{-1} in order to eliminate any thermal history. In the case of samples crystallized from the melt the samples were then quickly cooled to the preset crystallization temperature to initiate the isothermal crystallization. In the case of samples crystallized from the amorphous solid state, the samples were quickly taken out of the DSC cell and immediately quenched in liquid nitrogen. After submersion in liquid nitrogen for 5 min, the samples were transferred to the DSC which was set at the appropriate isothermal crystallization temperature. In both types of isothermal crystallization studies the samples were held at the crystallization temperature until no changes in the heat flow were observed.

Based upon the enthalpy evolved during crystallization the kinetics of crystallization was evaluated. The determination of time t=0 for the isothermal kinetic analysis was an issue of concern, especially for samples crystallized from the melt when fast crystallization rates were encountered. In an attempt to overcome this problem and prevent under shooting the desired isothermal crystallization temperature a procedure was developed to minimize the time required to achieve the stable desired temperature. This involved developing a programmed cooling profile which jumped to a temperature 5°C above the desired value followed by two controlled ramps, the first at 20°C min^{-1} to 2°C above the desired value followed by a second at 5°C min^{-1} to the desired isothermal temperature.

In addition the thermal stability of the samples was examined in a separate set of experiments. In these experiments the procedure described above for the isothermal crystallization studies from the melt were used, except that the samples were held at a temperature of 200°C for 0, 30 and 60 min prior to the rapid cooling to the melt isothermal crystallization temperature.

Results and discussion

Figure 2 shows the DSC traces for both the original polylactic acid sample and its nanocomposite following heating to 200°C and subsequent quenching in liquid nitrogen. It will be noted that both samples are characterized by a glass transition temperature (T_g), crystallization peak (T_c) and melting peak (T_m), typical of semi-crystalline polymers. The values for these transitions along with measured endotherms and exotherms are recorded in Table 1. Also listed in this table are estimates of the degree of crystallinity of these two samples (χ%) calculated using a value of 87 J g^{-1} for the heat of fusion of the pure PLLA crystal [7].

The development of the crystallinity in the two samples was monitored by the evolution of the heat released during the actual crystallization process. Figure 3 presents data for the isothermal crystallization of the neat PLA rapidly cooled from the melt. A similar set of DSC traces were obtained for the nanocomposite material. In both cases as the difference between the melting and crystallization temperature, decreased, the rate of crystallization got slower and the exothermal peak became broader and the time

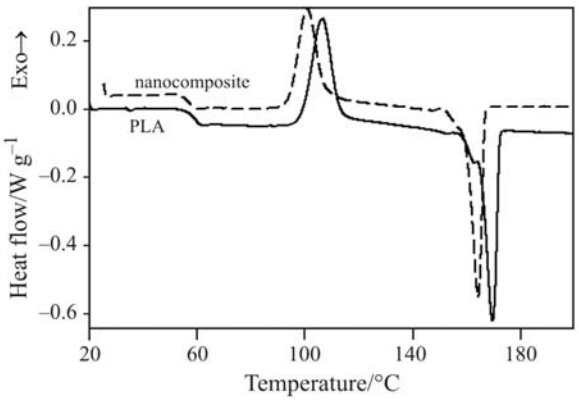

Fig. 2 DSC curves for the neat PLA and its nanocomposite following a rapid quench after being heated to 200°C

Table 1 Thermal characteristics of the samples evaluated as determined by DSC

Sample	T_g/°C	T_c/°C	ΔH_c/J g^{-1}	T_m/°C	ΔH_c/J g^{-1}	χ/%
Neat PLA	60.35	104.59	39.46	169.41	36.74	42.22
Nanocomposite	58.11	100.28	34.57	164.35	33.47	38.47

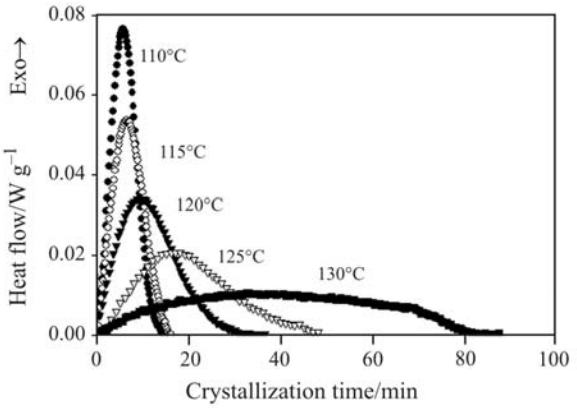

Fig. 3 DSC curves of the isothermal crystallization of the neat PLA samples cooled from the melt at various temperatures

to reach the peak value increased. While the appearance of the DSC traces for the neat polymer and the nanocomposite material were very similar, major differences were noted in the isothermal crystallization temperatures required to obtain meaningful scientific data. For example in the case of the neat PLA the isothermal crystallizations were measured over the range 105–130°C, while a temperature range of 120–150°C was used for the nanocomposite material. Similar traces were obtained for samples crystallized from the amorphous solid state, except in this case the temperature ranges used to follow the isothermal crystallization were almost the same (i.e. 80–110°C).

This data for the isothermal crystallization from the melt and the amorphous solid state is summarized in Table 2, where t_{max} represents the time to reach the maximum rate of heat flow while t_c represents the total crystallization time, after which no further heat flow was observed. Also listed in Table 2 are the values calculated for the total degree of crystallinity developed χ_c at t_c calculated once again using a value of 87 J g^{-1} for the heat of fusion of the pure PLLA crystal [7], along with calculated values for the relative crystallinity χ_{rel} at t_{max} calculated using χ_{max}/χ_c. From this data it would appear that while the overall degree of crystallinity achieved by the neat PLA and the nanocomposite samples are similar, irrespective of whether crystallized from the melt or from the amorphous solid state, the values obtained from the

Table 2 Relative and absolute crystallinities at t_{max} and t_c

Sample	T/°C	t_{max}/s	t_c/s	χ_c/%	χ_{rel}/%
Crystallization from the melt neat PLA	105.4	260	684	31.4	44.4
	110.4	330	912	35.3	47.5
	115.4	395	1070	33.1	45.6
	120.4	592	2220	36.7	41.7
	125.4	1040	4500	46.1	35.6
	130.4	1980	8400	44.4	37.8
Composite	120.4	41	150	24.7	32.1
	125.4	45	186	35.6	28.0
	130.5	65	248	41.4	41.0
	135.5	80	330	34.4	29.5
	140.5	182	660	43.0	38.8
	145.5	407	1470	47.9	42.5
	150.5	829	3060	49.2	36.3
Crystallization from the solid neat PLA	85.4	503	4290	30.9	39.4
	90.4	319	1310	31.2	43.3
	95.5	163	580	32.3	42.2
	100.6	106	500	32.0	35.5
	105.6	87	440	36.8	44.1
Composite	80.4	607	4620	30.3	22.1
	85.5	220	1620	25.6	27.9
	90.5	164	790	27.4	35.4
	95.6	92	270	22.5	40.9
	100.7	84	300	35.4	43.2
	105.8	32	228	39.8	29.6
	110.8	23	171	39.3	24.0

melt appear to be consistently higher than those obtained from the amorphous solid state. However, when the relative amounts of crystallinity are compared at time t_{max}, the values for the nano composite samples are consistently lower than those obtained for the neat PLA. This suggests that in the case of nanocomposite samples the impingement of the growing spherulite crystals occurs sooner than in the case of the neat PLA as shown by Blundell and Osborn [8].

The actual isothermal crystallization kinetics of the samples under various crystallization temperatures, as reported in Table 2, were actually determined using an Avrami analysis of the data [9, 10]. This makes use of the following expression which assumes that the evolution of the crystallinity is linearly proportional to the heat evolution which allows the relative degree of crystallinity, $X(t)$, to be obtained from these DSC curves.

$$X(t) = \frac{\int_0^t \frac{dH}{dt} dt}{\int_0^\infty \frac{dH}{dt} dt}$$

In this expression the first integral represents the heat generated at time t, while the second integral represents the total heat generated up to the end of the crystallization process. By equating the integrals to the areas of the isothermal DSC curves, the following equation is obtained:

$$X(t) = \frac{A_t}{A_\infty}$$

where A_t is the area under the DSC curves from t=0 to t=t and A_∞ is the total area under the crystallization curve. Using this equation, the mass fraction of the crystalline material [$X(t)$] at a specific time was calculated. Figure 4, illustrates the type of plots obtained for these values of $X(t)$ as a function of time for the neat PLA at the different melt crystallization temperatures used in this study. Once again similar plots were obtained for the PLA nanocomposite as well as samples crystallized from the amorphous solid-state.

The actual crystallization kinetic analysis of these systems is performed with the following Avrami equation:

$$X(t) = 1 - \exp(-kt^n)$$

where n is a constant that depends on both the nucleation and growth of the crystals and is normally an integer between 1 and 4 depending upon the crystallization mechanisms. By taking logarithms this equation takes the following form:

$$\log\{-\ln[1 - X(t)]\} = n\log t + \log k$$

which allows k and n to be determined from a plot of $\log\{-\ln[1-X(t)]\}$ *vs.* $\log t$.

These plots are shown in Fig. 5 for the neat PLA crystallized at several isothermal temperatures. Similar plots were obtained for the PLA nanocomposite sample as well as from both samples crystallized from the amorphous solid state. For the sake of repeatability and consistency only the crystallization data between 5 and 70% was used to calculate the values for n and k. This helped to remove any possible uncertainties that could be introduced by using values greater than 70% where deviation from linearity is possible due to secondary crystallization [11, 12].

The values for n and k calculated from these plots are summarized in Table 3. It is well known that the value of n depends on both the mechanism of nucleation and crystal growth, and usually is an integer between 1 and 4. The n values found in this study were all in the vicinity of 2 and appeared to be independent of the presence or absence of the nano clay particles, or whether the crystallization was from the melt or the amorphous solid state. This value for the Avrami exponent suggests that the crystallization

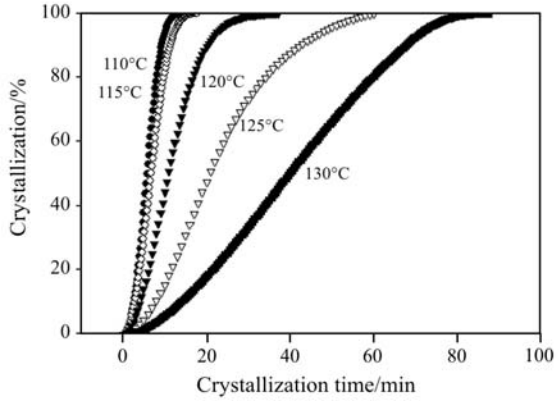

Fig. 4 Plots of the relative crystallinity *vs.* time for the neat PLA samples cooled from the melt at various isothermal crystallization temperatures

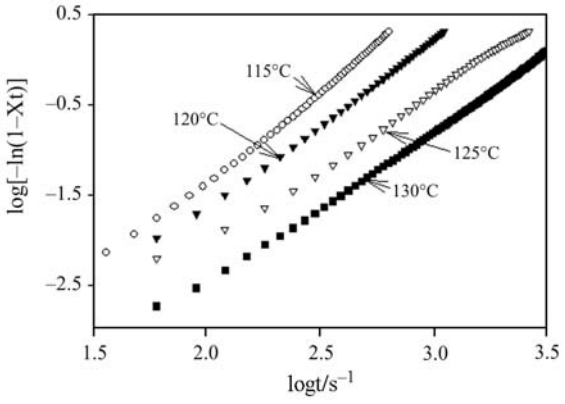

Fig. 5 Avrami plots of $\log[-\ln(1-Xt)]$ *vs.* $\log t$ for the neat PLA samples cooled from the melt at various isothermal crystallization temperatures

Table 3 Results of the Avrami analysis

Crystallization from the glass				
Sample	Xst T/°C	n	log$k$/s^{-1}	$t_{1/2}$/s
PLA	85.4	2.24	–6.4048	614
	90.4	2.20	–5.7703	355
	95.5	2.53	–5.9492	194
	100.6	2.69	–5.8333	129
	105.6	2.38	–5.0837	117
Composite	80.4	1.98	–6.1491	1060
	85.5	2.14	–5.5258	322
	90.5	2.19	–5.2245	206
	95.6	2.58	–5.3310	101
	100.7	1.80	–3.7310	96
	105.8	1.79	–3.1810	49
	110.8	1.81	–3.0388	39
Crystallization from the melt				
Sample	Xst T/°C	n	log$k$/s^{-1}	$t_{1/2}$/s
PLA	105.4	2.07	–5.2615	292
	110.4	2.18	–5.7615	371
	115.4	1.97	–5.3202	417
	120.4	1.90	–5.4866	637
	125.4	1.82	–5.8325	1310
	130.4	1.71	–5.9433	2413
Composite	120.4	2.51	–4.4679	52
	125.4	2.44	–4.5397	62
	130.5	2.21	–4.5749	100
	135.5	2.52	–5.2085	101
	140.5	2.08	–5.0174	217
	145.5	2.00	–5.4446	439
	150.5	1.96	–6.1211	1101

mechanism is a two-dimensional growth process with possibly some thermal and athermal nucleation (i.e. instantaneous and sporadic nucleation mechanisms) [13]. The values of n and k obtained from these Avrami plots were then used to calculate the crystallization half times, $t_{1/2}$, defined as the time required for half of the final crystallinity to develop. These values are also shown in Table 3 and have been plotted as a function of crystallization temperature T_c, in Fig. 6. From the data shown in this figure the strong dependence of $t_{1/2}$ on the crystallization temperature was evident. For samples crystallized from the melt the crystallization half time, $t_{1/2}$ increases with increase in the crystallization temperature, while the reverse effect was observed with samples crystallized from the amorphous solid state. Furthermore, it is clearly evident that for a given crystallization temperature the nanocomposite sample has a lower $t_{1/2}$ value than the

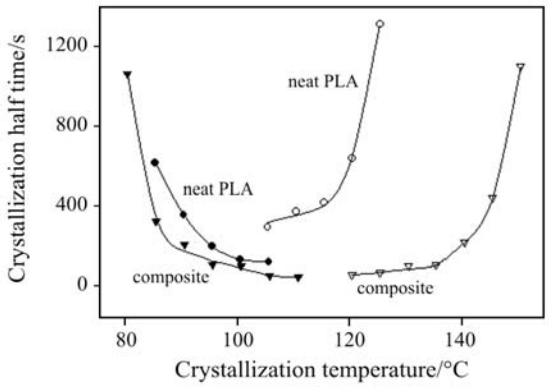

Fig. 6 Crystallization half times as a function of isothermal crystallization temperature for the neat PLA and composite samples

neat PLA polymer. This indicates that the pure PLA has a slower crystallization rate (lower $t_{1/2}$) than that found with the composite sample. For example, if the $t_{1/2}$ values for the composite and neat PLA are compared using the crystallization temperatures of 120, 125 and 130°C for comparison purposes (data from Table 3) it would appear that the presence of the nanoclay particles in the PLA causes the crystallization rate of the neat PLA to increase by a factor of about 19. Although different experimental approaches were used to determine the crystallization kinetics from the melt and the amorphous solid it would appear that based upon the data presented in Fig. 6 that the maximum crystallization rate (lowest $t_{1/2}$ value) for the neat PLA is around 105°C. Meanwhile in the case of the composite sample the crystallization rate maximum (lowest $t_{1/2}$ value) is less well defined, although it would appear to be in the range of 105 to 125°C.

Based upon this evidence it is clear that the crystallization rate for this polymer is going to be heavily dependent upon the presence of the nano clay particles which appear to be acting as nucleating agents. This factor is going to greatly effect the processing of these materials, especially for our interest in the production of foamed composites from these materials. This situation arises because in the case of the production of cellular foamed materials it is known that the presence of nucleating agents such as nano clay particles can greatly influence the rate of cellular nucleation, accelerating the process as the amount of particular matter increases [14]. However, based upon the results obtained in this current study it is also clear that these same nanoparticles increase the crystallization rate. This raises an interesting dilemma since it is known that in the case of foaming a polymer with supercritical CO_2 the process is very much dependent upon the solubility of the CO_2 in the amorphous region of the polymer (the CO_2 does not penetrate the crystalline region) [15, 16]. Consequently, in order to ensure the sat-

isfactory foaming of these nanocomposites it is essential to know how the rates of crystallization and the rate of cellular foam nucleation compare.

The processing of polymeric thermoplastics involves holding the samples at elevated temperatures for several minutes. In order to determine the possible effect of this heating on the isothermal crystallization kinetics, some simple thermal exposure experiments were conducted in the DSC cells. These experiments involved heating the samples at 200°C for 0, 30 and 60 min. Following these heating periods the isothermal crystallization kinetics were followed by rapidly cooling the samples from the melt to the desired isothermal temperature. Once again the DSC results were analyzed by the Avrami expression and the results are summarized in Table 4.

From this data it would appear that the crystallization kinetics of both the neat PLA and the nanocomposite are affected to some extent by holding the samples at 200°C. However, the kinetic effects are not the same for each sample, as can be seen from the plots of representative data obtained for the neat PLA at a crystallization temperature of 110°C and the nanocomposite at a crystallization temperature of 140°C as shown in Fig. 7. Clearly, based upon this data, it would appear that holding the sample at a temperature of 200°C enhances the rate of crystallization of the pure PLA while reducing that of the nanocomposite material. The rationalization for this contrary phenomenon is uncertain although in the case of the neat PLA it can be speculated that the heating at 200°C causes the possible formation of nucleating sites in the polymer melt, which increase with hold time. These new and increased numbers of nucleating sites are then able to facilitate the nucleation and growth of the crystalline domains in the neat polymer. Meanwhile in the case of the nanocomposite material the nano clay particles already provide the polymer with a large number of nucleating sites that facilitate the growth of the crystalline domains. Consequently an increase in the rate of crystallization is not to be expected. However, the observation that the actual rate of crystallization of the nanocomposite is retarded suggests that changes are taking place within the polymer, or at the polymer clay interface which slow down the actual nucleation and/or growth of the crystalline domain within the composite material.

In addition to measuring the crystallization kinetics of samples heated at 200°C it was also decided to investigate the effect of these exposures on the T_g, crystallization and melting of quenched samples after heating for periods of 0, 30 and 60 min. These results are summarized in Table 5. Based upon this data it would appear that holding the neat PLA at 200°C for times up to 60 min has a negligible effect on any of these values. However, in the case of the nanocomposite material changes were noted in all properties measured. For example in the case of the glass transition temperature of the nanocomposite there was a slight increase in this value with increasing hold time at 200°C.

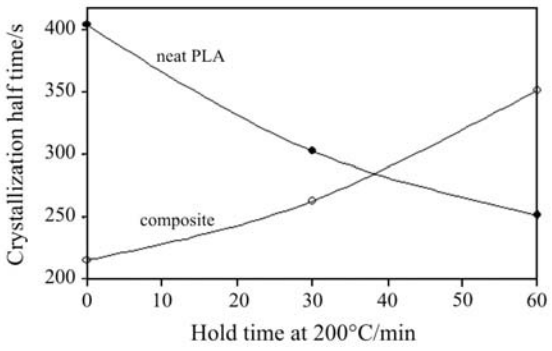

Fig. 7 Crystallization half times for neat PLA and the nanocomposite at a crystallization temperature of 110 and 140°C, respectively after holding the samples at 200°C for different times

Table 4 Results of the Avrami analysis of samples heated at 200°C and crystallized from the melt

Sample	Xst T/°C	0 min at 200°C			30 min at 200°C			60 min at 200°C		
		n	log$k$/s^{-1}	$t_{1/2}$/s	n	log$k$/s^{-1}	$t_{1/2}$/s	n	log$k$/s^{-1}	$t_{1/2}$/s
PLA	105.4	2.07	–5.2615	292	1.81	–4.3838	215.8	2.06	–4.9381	210
	110.4	2.18	–5.7615	371	2.07	–5.2949	302.7	2.05	–5.0813	252
	115.4	1.97	–5.3202	417	1.93	–5.0587	345.6	1.93	–5.1867	398
	120.4	1.90	–5.4866	637	1.86	–5.3865	646.3	1.97	–5.5720	566
	125.4	1.82	–5.8325	1310	1.68	–5.4418	1394.6	1.79	–5.6128	1123
Composite	120.4	2.51	–4.4679	52	1.87	–3.8800	97.1	2.17	–4.7598	133
	125.4	2.44	–4.5397	62	2.48	–5.2120	108.9	2.30	–5.0841	138
	130.5	2.21	–4.5749	100	2.28	–5.0824	145.0	1.99	–4.5850	167
	135.5	2.52	–5.2085	101	1.67	–3.7904	149.6	1.98	–4.8143	225
	140.5	2.08	–5.0174	217	1.94	–4.8591	263.5	1.77	–4.6752	351
	145.5	2.00	–5.4446	439	1.97	–5.5873	571.7	1.81	–5.3113	702

Table 5 Thermal characteristics of samples heated at 200°C

Sample	T_g	Crystallization peak		Melting peak	
	temp./°C	temp./°C	area/J g^{-1}	temp./°C	area/J g^{-1}
Neat PLA					
0 min at 200°C	60.4	104.6	39.46	169.4	36.74
30 min at 200°C	59.9	104.0	40.57	169.3	36.92
60 min at 200°C	60.4	104.5	40.67	169.1	37.62
Composite					
0 min at 200°C	58.1	100.3	34.57	164.4	33.47
30 min at 200°C	58.6	104.3	35.38	165.0	33.98
60 min at 200°C	59.2	106.7	38.38	165.2	36.58

Although the increase was small it was repeatable. Similar increases were also noted for the peak crystallization temperature and peak melting temperatures. Both changes suggest a delay in the crystallization process as a result of the thermal exposure, consistent with the observed decrease in the crystallization kinetics. However, a more interesting observation was the apparent increase in the crystallizability of the composite samples associated with the heating as reflected in the measured heats of crystallization and fusion. The rationalization of this apparent increase in crystallizability appears contrary to expectations.

Conclusions

PLA and its nanocomposite with clay have been shown to follow an Avrami behaviour during isothermal crystallization from the melt and from the amorphous solid state. The Avrami exponents '*n*' in all cases were about two. The values for the crystallization half-times show that the isothermal crystallization rate of PLA is greatly enhanced by the presence of nano clay particles within the matrix, especially when crystallized from the melt as would be the case under conventional processing conditions. For example when the materials were crystallized from the melt in the temperature range from 120–130°C the crystallization rate for the composite material was approximately 15 to 20 times faster than that for the neat PLA. Meanwhile in both cases the maximum crystallization rates observed were in the region of 105–125°C, with that for the neat PLA being closer to 105°C. It was also interesting to note that prolonged heating at 200°C for times up to 60 min affected the crystallization behaviour of the two samples in completely different manners. For example the crystallization rate for the neat PLA was noted to increase with prolonged exposure at 200°C, while the rate for the composite sample was noted to decrease.

Acknowledgements

The authors wish to thank Dr. Kauze Ueda at Unitika Ltd. for her kind assistance with the materials used in this study.

References

1 National Research Council, Ed., 'Biobased Industrial Products; Priorities for Research and Commercialization' Washington D.C. 2000.
2 H. Tsuji, 'Polylactides', in: Biopolymers. Polyesters III. Applications and Commercial Products, 1st Edition, Y. Doi, A. Steinbüchel, Eds, Wiley-VCH Verlag GmbH, Weinheim 2002, pp. 129–177.
3 M. Naitove, Plast. Technol., 44 (1998) 13.
4 R. E. Drumright, P. R. Gruber and D. E. Henton, Adv. Mater., 2 (2000) 1841.
5 D. Schmidt, D. Shah and E. P. Giannelis, Curr. Opin. Solid State Mater. Sci., 6 (2002) 605.
6 Y. Di, S. Iannace, E. di Maio and L. Nicolais, J. Polym. Sci. Part B: Polym. Phys., 43 (2005) 689.
7 E. W. Fischer, H. J. Sterzel and G. Wegner, Koll.-Z. Z. Polym., 251 (1973) 83.
8 D. J. Blundell and B. N. Osborn, Polymer, 24 (1983) 953.
9 M. J. Avrami, Chem. Phys., 7 (1934) 1103.
10 M. J. Avrami, Chem. Phys., 8 (1940) 212.
11 P. Cebe and S. D. Hong, Polymer, 27 (1986) 1183.
12 Y. Lee and R. S. Porter, Macromolecules, 21 (1988) 2770.
13 B. Wunderlich, Macromolecular Physics, Vol. 2, Academic Press, New York 1976, p. 132.
14 N. S. Ramesh, D. H. Rasmussen and G. A. Campbell, Polym. Eng. Sci., 34 (1994) 1685.
15 Y. P. Handa, Z. Zhang and B. Wong, Macromolecules, 30 (1997) 8499.
16 Z. Zhang and Y. P. Handa, Macromolecules, 30 (1997) 8505.

CTAS 2005
OnlineFirst: October 20, 2006

DOI: 10.1007/s10973-006-7717-9